



An evolutionary game with revengers and sufferers on complex networks



Yuji Zhang, Ziyuan Zeng, Bin Pi, Minyu Feng*

College of Artificial Intelligence, Southwest University, Chongqing 400715, PR China

ARTICLE INFO

Article history:

Received 27 February 2023

Revised 29 April 2023

Accepted 2 June 2023

Keywords:

Evolutionary game

Revenge and suffer

Network science

Cooperation

ABSTRACT

The networked evolutionary game theory makes investigations on how the emergence of cooperative behaviors in the real world possible. Many researches based on costly punishment have found profound achievements. However, the order of punishment and timely update of payoff in the process of punishment do not get much attention. Therefore, based on the above deficiencies, we study a revenge-based prisoner's dilemma game on square-lattice and small-world networks to explore how it affects the emergence and maintenance of cooperation behaviors on complex networks. In simulations, we exhibit the evolution of the cooperation frequency as the population processes and probe the effects of the loss function, the number of players updating strategies, the cost-to-benefit ratio, and network size on the cooperation frequency, and further demonstrate the evolution of the number of revengers and sufferers over time, which may help to understand the role of them played in networks. By varying corresponding revenge parameters, our proposed mechanism helps to overcome social dilemmas. Moreover, we find the phenomenon that the cooperation frequency declines and then rises in small-world networks under certain conditions, which we validate from the variance of the numbers of revengers and sufferers over time. Our work may help to illuminate the study of evolutionary games with revengers and sufferers.

© 2023 Elsevier Inc. All rights reserved.

1. Introduction

According to the theory of evolution proposed by Darwin [1], cooperation can not be maintained in nature and human societies, and defection to maximize one's payoff seems like the best strategy. However, group cooperation widely prevails in reality, which is a conundrum troubling researchers and is also a challenge attracting those from different disciplines to explore the potential reasons [2,3]. Game theory in complex networks has provided a theoretical and powerful tool to probe into the puzzle. The prisoner's dilemma game (PDG) [4,5], snowdrift game (SDG) [6,7], and public goods game (PGG) [8,9] have been intensely studied in homogeneous networks (e.g., square-lattice networks [10,11] and small-world networks [12,13]) and heterogeneous networks (e.g., scale-free networks [14,15]). To better approximate and simulate the real world, researchers are dedicated to improving existing networks and proposing novel networks [16,17]. In networks, a node represents a player, i.e., each player occupies one node, and links between different nodes reveal the interaction between players (players having interactions called neighbors). Connected players play a game with their neighbors to gain a payoff determined by bilateral strategies. Generally, different kinds of game models and the topology of networks have a strong influ-

* Corresponding author.

E-mail address: myfeng@swu.edu.cn (M. Feng).

ence on the evolution of cooperation [18]. Nowak proposed five renowned rules in 2006 [19], i.e., kin selection [20], direct reciprocity [21], indirect reciprocity [22], group selection [23], and network reciprocity [24,25], which effectively boost cooperation. In addition, Ohtsuki et al. proposed a general and simple rule for the evolution of cooperation on specific graphs [26]. Mechanisms like reward [27], contact pattern [28], conformists and profiteers [29,30], interaction lifespans [31] and so on [32,33], which are abstracted from reality, have also been verified to be beneficial to the emergence of cooperation. Furthermore, cooperation in dynamic networks (e.g., temporal networks [34]), higher-order networks [35], and multilayer networks [36] have been deeply and widely investigated.

The punishment-based mechanism has been widely explored [37,38], where the core of it is the decrease of the punished individuals' payoff, which has been verified to promote cooperation effectively. For example, Song et al. proposed a conditional neutral punishment mechanism where a player punishes its neighbors with the opposite strategy when its payoff is lower than the average payoff of its neighbors [39]. Wang and Guo put forward a new strategy that combines punishment and extortion used by one leader in scale-free networks [40]. Further, on the basis of the bilateral cost, costly (or altruistic) punishment attracted researchers' attention [41,42], of which the feature is that the basic prisoner's dilemma game is extended from two strategies, cooperation (C) and defection (D), to three, i.e., C , D , and punishment (P) [43]. Moreover, numerous researchers have achieved striking achievements in the mechanism mentioned. For instance, Wang et al. studied the effects of wealth-based rule in costly public goods games when individual selection is inevitable [44]. Mieth et al. examined the effects of a moral-framing manipulation in the prisoner's dilemma game with a costly punishment option [45].

As described above, numerous novel and innovative ideas about (costly) punishment have been proposed. However, we think the payoff gained in each round has an influence on the results of costly punishment to simulate some complex phenomena of punishment or revenge in society. Thus, in light of the points previously mentioned, in this study, based on the concept of the costly punishment mechanism, we extend it to get the revenge mechanism. As we know, acts of revenge widely exist in society, which is especially outstanding between companies, countries, and etcetera, and Jon Elster proposed the norms of revenge in 1990 [46]. Moreover, the well-known strategy, tit for tat, is also a form of revenge in the sense of strategy, where one player starts with cooperation and then imitates its opponent's previous strategy [47]. Nowak and Sigmund proposed the generous tit for tat, which is more beneficial to cooperation, compared to tit for tat [48]. In reality, the game between companies is not in the minority, and in the backdrop of globalization, two companies related in affairs often choose to cooperate for a mutual and lucrative payoff. However, since unpredictable and capricious situations, e.g., sometimes they are at loggerheads over the share of profits, cooperation can not always be sustained, i.e., one decides to defect unilaterally. Usually, canceling the partnership and turning to defection is not enough, i.e., they would take further action such as revenge, where both suffer since the breakdown of cooperation. The novel mechanism follows the traditional PDG setting, where two behaviors (C and D) are available. Besides, we assume that in each round, players remember the information from the last round, which impacts the conduct of revenge. The condition for costly punishment is different from the conventional punishment model where the punishment is a strategy like cooperation and defection, and the proposed mechanism is more focused on the costly punishment for violating mutual cooperation. Furthermore, different from the costly punishment mechanism where a new behavior (punishment) is added, the new mechanism allows players to revenge after each round, and the bilateral cost is flexible, i.e., we suppose that it depends on the loss function related to the revenger's current payoff, which is more in line with reality. We take the order of punishment into consideration. The reasons are given as follows: from a temporal perspective, we suppose the punishment cannot be completed at the same time. The order of punishment indicates that after each punishment, the original payoff of the revenger decreases, which directly influences the punishment on the next player. Considering to simulate the connection between different people in society, we investigate our model on square-lattice networks, and small-world networks, where the player plays a game with its neighbors. We explore how the revenge mechanism affects the variation of cooperation frequency in complex networks, and relevant results obtained via simulation indicate that the new mechanism effectively prompts cooperation behaviors in the square-lattice networks and small-world networks.

The organization of this study is given below. In Section 2, we detail our model, including the rule of the revenge mechanism, the strategy-updating rule, and the calculation of players' payoff. In the next section, we sketch out simulation methods, present relevant simulation results, and uncover the hidden information in our results. Eventually, we conclude our work and give the prospect in the last section.

2. Model

In this section, we primarily give elaborate illustrations of our model in accordance with the revenge mechanism, including the calculation of different types of players' payoff, the strategy-updating rule, and the revenge mechanism.

2.1. Background

In this paper, we take the dynamic evolution in PDG into consideration for our proposed model. For that purpose, we briefly depict the original PDG model where players have two optional strategies, including cooperation (C) and defection (D). If two players choose to cooperate, then both of them derive the same reward (R); however, for mutual defection, they obtain the same punishment (P). Moreover, for two opposite strategies, the unilateral cooperator gets the sucker's payoff (S), while the other adopting defection receives the temptation (T). Besides, in the PDG, R , P , S and T satisfy the following

conditions: $T > R > P > S$ and $2R \geq T + S$. For simplicity, we set $R = 1$, $P = 0$, $S = -r$, and $T = 1 + r$, where r represents the cost-to-benefit ratio and $0 < r \leq 1$ is a regulable parameter. For an individual, defection is always the best strategy no matter what strategy the opponent adopts, i.e., (D, D) is the Nash equilibrium in a well-mixed population. The matrix of players' payoff in PDG is:

$$\begin{matrix} & \begin{matrix} C & D \end{matrix} \\ \begin{matrix} C \\ D \end{matrix} & \begin{pmatrix} 1 & -r \\ 1+r & 0 \end{pmatrix} \end{matrix} \quad (1)$$

2.2. Strategy evolution

Hereby, we give a concise introduction to the dynamic evolution. We suppose that N players exist in a given network, and each player occupies a node in the specified network, which is randomly initialized to a cooperator or a defector with the probability 50% respectively. In each round, each player can only be a cooperator or defector, then plays games with all its neighbors and obtains relevant payoff according to the payoff matrix shown in Eq.(1). At the end of each round, p ($0 < p \leq 1$) percentage of players are randomly chosen to update their strategies, which is different from many other models where all players update their strategies in each round. The reason for only part of the players updating their strategies is that, in reality, part of the players may be in an inactive state, where they keep their original strategies unchanged. Furthermore, we will exhibit the relevant simulation results for further elucidation in the next section. Chosen players imitate a reference player who is selected randomly from its neighbors with a probability, which is calculated by the Fermi function:

$$P(s_x \leftarrow s_y) = \frac{1}{1 + \exp[(\Pi_x - \Pi_y)/\kappa]}, \quad (2)$$

where s_x , Π_x , and κ represent the player x 's strategy, x 's payoff, and the rationality of the player respectively. Specifically, Eq. 2 states that more differences between x 's and y 's payoff make it more possible that x takes y 's strategy and vice versa. For simplicity, we set $\kappa = 1$. After the strategy update, each player decides whether to retaliate depending on its neighbors' strategy change, of which details will be mentioned in the next subsection.

2.3. Revenge mechanism with punishment order

We suppose that a structured population comprises two types of players: cooperators and defectors, who take cooperation or defection as the game strategy. As time evolves, the strategies of different players vary. It is known that mutual cooperation is exactly what people, in reality, are pursuing, which helps to solve social dilemmas. Hereby, we give the conditions for the emergence of revengers and sufferers. At the time t , for player i and j , if $s_i = s_j = C$ and $s_i = C, s_j = D$ at the next time step, then i will carry out the execution of revenge on j . We can interpret the reason for i 's such behavior as j against i 's willingness to continue cooperating, which enrages i or i is selfish, which leads to the punishment. The revenge is focused on behavior outside of the game, different from the game strategy, which can be learned by other players. Moreover, from a temporal perspective, we suppose the punishment cannot be completed at the same time, i.e., there exists the order of punishment. The order of the punishment practically indicates that players can no longer afford to maintain the original punishment strength as the number of punishments increases, i.e., players who are punished later lose less than players who are punished first. We have to point out that we just consider such behavior in an ideal state and it just exists in the model for research.

Meanwhile, the revenger can not "keep out of the affair", i.e., the necessary cost is inevitable. In addition, if one's current payoff is less than 0, it can not execute the aforementioned revenge. For the loss function of both sides, we assume that the quantity of the loss of a revenger and sufferer depends on the revenger's payoff obtained from the current round. Therefore, we introduce two scale parameters ρ_r and ρ_s (both from 0 to 1), representing the loss ratio of the revenger and sufferer in each conduct of revenge respectively. We denote $\Pi_i^{(1)}$ as the payoff of player i calculated by the payoff matrix, i.e.,

$$\Pi_i = \begin{cases} \sum_{j \in \mathcal{Q}, s_j=C} (1) + \sum_{j \in \mathcal{Q}, s_j=D} (-r) & , \text{if } s_i = C \\ \sum_{j \in \mathcal{Q}, s_j=C} (1+r) & , \text{if } s_i = D \end{cases} \quad (3)$$

where \mathcal{Q} indicates the set of the neighbors of i and s_i denotes the strategy of i . Next, based on Eq. 3, for a revenger α , we assume that n players are the target of α , i.e., for j th and $(j+1)$ th sufferer ($1 \leq j \leq n-1$) the recursive expressions formula of α 's payoff is $\Pi_{\alpha}^{<j+1>} = (1 - \rho_r) \Pi_{\alpha}^{<j>}$. Therefore we can derive the payoff of α after the revenge on n players, i.e., $\Pi_{\alpha}^{<n>} = (1 - \rho_r)^n \Pi_{\alpha}$. Similarly, for a sufferer β , we assume that it is the target of m revengers, thus we can obtain the payoff of β , i.e., $\Pi_{\beta}^{(m)} = \Pi_{\beta} - \sum_{i=1}^m \rho_s \Pi_i^{<f(\beta,i)-1>}$, where $f(\beta, i)$ denoting β is the $f(\beta, i)$ th revenge target of i (specifically, $\Pi_i^{<0>} = \Pi_i$). We utilize two symbols $<>$ and $()$ to distinguish the payoff of revengers and sufferers respectively. Concerning the order of revenge in simulations, it follows the rule that in the generation of the specific network, each node is labeled with a number, which determines the order of revenge. That is to say, the node labeled with a small number will be revenged earlier than larger nodes in each execution of revenge.

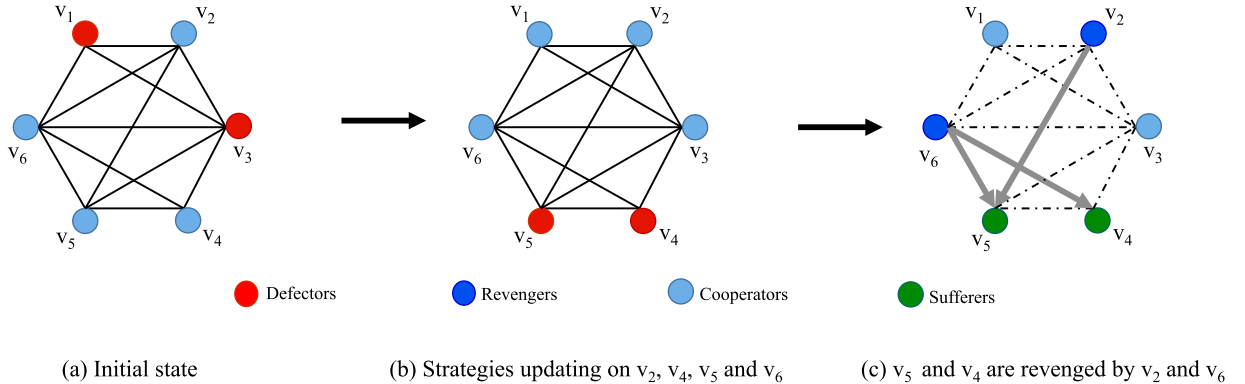


Fig. 1. Illustration of the model. This figure shows how the revenge mechanism works in a randomly generated small-world network, where the light blue, red, dark blue, and green nodes are cooperators, defectors, revengers, and sufferers respectively. In subplot (a), (V_2, V_5) , (V_2, V_6) , (V_4, V_5) , (V_4, V_6) and (V_5, V_6) take mutual cooperation where they gain R . In subplot (b), V_4 and V_5 update their strategies shifting from C to D according to Eq. 2, and V_2 and V_6 remain their cooperation strategies unchanged. Considering the defection of V_4 and V_5 , which makes the payoff of V_2 and V_6 switch from R to S , V_2 and V_6 are revenged on V_5 and V_6 are revenged on V_4 (shown by the bold arrows), i.e., V_2 and V_6 are revengers, and V_4 and V_5 are the sufferers in the current round shown in subplot (c), according to the conditions of the revenge mechanism. V_4 will be punished before V_5 facing V_6 's revenge. In subplot(b), the payoff of V_2 , V_4 , V_5 and V_6 is $\Pi_{V_2} = 3 - r$, $\Pi_{V_4} = 2 + 2r$, $\Pi_{V_5} = 3 + 3r$ and $\Pi_{V_6} = 3 - 2r$ respectively. In subplot(c), the payoff of V_2 , V_4 , V_5 and V_6 is $\Pi_{V_2}^{<1>} = (1 - \rho_r)\Pi_{V_2}$, $\Pi_{V_4}^{(1)} = \Pi_{V_4} - \rho_s\Pi_{V_6}$, $\Pi_{V_5}^{(2)} = \Pi_{V_5} - \rho_s(\Pi_{V_2} + \Pi_{V_6}^{<1>})$ and $\Pi_{V_6}^{<2>} = (1 - \rho_r)^2\Pi_{V_6}$ (after punishing V_4 , $\Pi_{V_6}^{<1>} = (1 - \rho_r)\Pi_{V_6}$ respectively, where $f(V_5, V_2) = 1$, $f(V_4, V_6) = 1$ and $f(V_5, V_6) = 2$.

To better clarify our model, we briefly conclude the modeling section. First, we introduce the contents and payoff matrix of traditional PDG, then give the strategy-updating rule (the Fermi function), and describe the details of the revenge mechanism. Fig. 1 provides an intuitive exhibition of our model in a randomly generated small-world network. In the next section, we will illustrate the simulation results attached to their analyses.

3. Methods, results and analyses

In this section, we depict the process of the simulation methods and exhibit the results derived from simulations together with relevant analyses. It is known that the square-lattice network (SL) has a simple network structure where each node has the same degree, and the small-world network (WS) well simulates the phenomenon of six degrees of separation, which widely exists in reality. Therefore, simulation results are obtained in SL and WS. Specifically, we analyze the evolution of f_c over time under different values of (ρ_r, ρ_s) . Subsequently, we exhibit the variation of f_c under different r , which determines the strength of PDG. Next, we give the variance of the number of revengers and sufferers under different p , which may uncover their function during evolution. Finally, we allow the network size N to vary over a relatively large range to examine the robustness of our model.

3.1. Methods

In the initial stage of each simulation, $N = 1600$ players are embedded into a 40×40 square-lattice network (SL) or small-world network (WS), and different numbers of players will be considered in detail in subsection 3.6. *Frequency of cooperation affected by network size*. The square-lattice network has periodical boundary conditions that eliminate the distribution difference. The generation of the small-world network has three significant factors: the number of nodes (N), the random reconnection probability, and K (an even number), which means each node is linked to $K/2$ nodes in the initial state. All simulation results are derived over $T = 10^4$ time steps. Moreover, for accuracy and generality, we take the average 100 independent simulation results for each set of parameter values as the final simulation results.

3.2. Effect of parameter pair (ρ_r, ρ_s) on frequency of cooperation over time

The cooperation level usually intrigues and concerns people, and cooperation frequency f_c , as a commonly used indicator of it, indicates the proportion of cooperators. Thus, in our proposed model, we explore the evolutionary relationship of f_c with aspect to time t under different parameters ρ_r and ρ_s . We set $t = 10^4$, which assures that after a long time of evolution, the results of the cooperation frequency are stable and avoid sharp fluctuation. The results of f_c varying with t in SL and WS are shown in Fig. 2.

In each subfigure of Fig. 2, the phenomenon is observed in the initial state ($t < 100$, according to the results of the simulation, not obvious in Fig. 2), all curves exhibit the same trend and overlap together, i.e., during the initial evolutionary process, the effects of the revenge mechanism are not revealed yet. In Figs. 2(a) and 2(c), considering two different parameters ρ_r and ρ_s , we fix $\rho_s = 1$ and make ρ_r vary from 0.2 to 1 with step equals 0.2, and the traditional mechanism

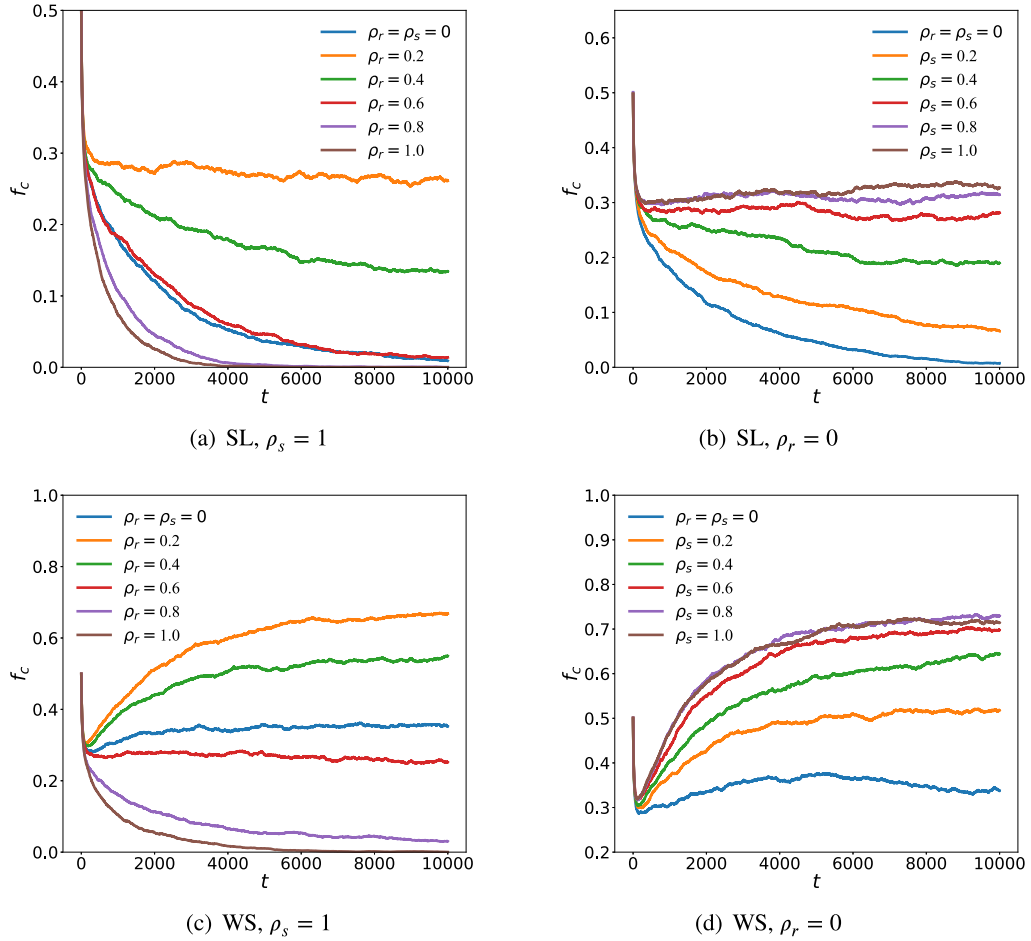


Fig. 2. Variance of frequency of cooperation against time. SL is a square-lattice network with $N = 40 \times 40$, and WS is formed by a small-world network with the reconnection probability is 0.3, the size of it is set as $N = 1600$ and $K = 4$. In Figs. 2(a) and 2(c), the parameter pairs (ρ_r, ρ_s) are set to $(0.2, 1)$, $(0.4, 1)$, $(0.6, 1)$, $(0.8, 1.0)$, $(1.0, 1.0)$, and $(0, 0)$ respectively. Analogously, the parameter pairs (ρ_r, ρ_s) in Figs. 2(b) and 2(d) are set to $(0, 1.0)$, $(0, 0.8)$, $(0, 0.6)$, $(0, 0.4)$, $(0, 0.2)$, and $(0, 0)$ respectively. The range of each x -axis is set within the interval $[0, 10^4]$, and y -axis of subplot (a), (b), (c), and (d) is set as $[0, 0.5]$, $[0, 0.65]$, $[0, 1.0]$ and $[0.2, 1.0]$ respectively. Additionally, the cost-to-benefit ratio r is set to 0.02 in the SL and 0.05 in the WS, and in each round, $p = 1$, i.e., 160 players are randomly chosen to update their strategies. We set the upper limit of the interval of t to 10^4 to obtain stable results of the cooperation frequency.

$(\rho_r = \rho_s = 0)$ is added as a control group. Figs. 2(a) and 2(c) indicate that with the increase of ρ_r , i.e., the relative cost of each revenge increases, the rate of cooperation decreases. In Fig. 2(a), for $\rho_r = 0.2$, there exists a turning point, after which the rate of decline slows down. Similar results, i.e., the existence of turning points in the curves, are observed in the other three subplots. Besides, when $\rho_r = 0.6$, the red curve almost overlaps the blue one, which uncovers that although revengers assume less cost than sufferers, its effect on the cooperation frequency is nearly the same as the traditional mechanism (the blue curve). Furthermore, f_c converges to 0 more rapidly when $\rho_r = 0.8$ and 1.0, compared to the traditional mechanism. We can interpret the phenomenon as there existing a “invisible upper bound”: if the cost of the revengers exceeds the bound, cooperation will disappear, though it punishes the mutinous defectors. In Fig. 2(c), for $\rho_r = 0.2$, the curve obviously shows a significant upward trend after around $t = 10^2$ (based on the results of the simulation, not obvious in Fig. 2(c)), although f_c first decreases from 0.5 to 0.3 and then rises to around 0.7. However, compared to WS in Fig. 2(c), all curves present a downward trend in SL in Fig. 2(a).

Then, in Figs. 2(b) and 2(d), we fix $\rho_r = 0$ and let ρ_s vary from 0.2 to 1 with step equals 0.2, i.e., the model degenerates into the traditional punishment model where punishers do not bear losses. Figs. 2(b) and 2(d) elucidate that with the rise of ρ_s , the rate of cooperation increases, and when $\rho_s = 0.8$ and 1.0, f_c maintains near 0.3 and 0.7 in SL and WS respectively. Analogously, it indicates that there exists a “lower bound”, which keeps the cooperation maintained at a steady level after sufficient time for evolution. In Fig. 2(b), for $\rho_s = 0.8$ and 1.0, f_c almost achieves the same results where it converges to 0.3. In Fig. 2(d), we get a similar result with slight differences where f_c converges to 0.7 and for all t , two curves ($\rho_s = 0.8$ and 1.0) are almost the same. In addition, for ρ_s varying from 0.6 to 1.0, a turning point strikingly raises the falling curve to around 0.7 at $t = 10^4$ in Fig. 2(d).

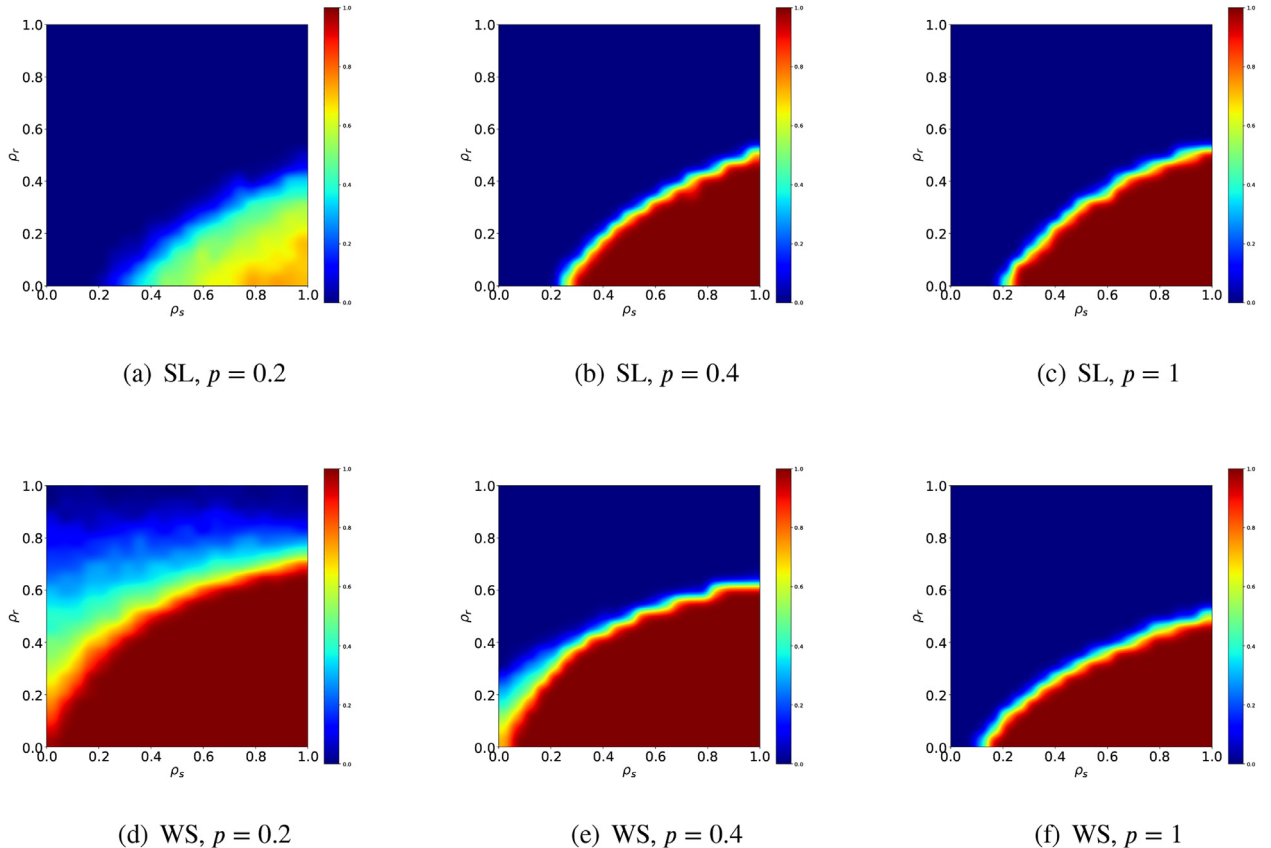


Fig. 3. The influence of parameter pairs (ρ_r, ρ_s) on cooperation behaviors. Heat maps of 320, 640, and 1600 players who update their strategies each round in the SL (subplots (a), (b), and (c)) and WS (subplots (d), (e), and (f)). The number of players is $N = 1600$ for two networks, and especially for the WS, the random reconnection probability is 0.3 and $K = 4$. Additionally, the parameter r is set as 0.02, and from left to right, p is set as 0.2, 0.4, and 1.0 respectively. The x-axis and y-axis represent ρ_s and ρ_r respectively, and the range of them is set to $[0, 1]$. We average 100 independent simulations as the final result, and each result is obtained from the averaged last 10 time steps.

3.3. Heatmaps of effect of parameter pair (ρ_r, ρ_s) on cooperation frequency

After deriving the variance of f_c against evolutionary time and some specific (ρ_r, ρ_s) , to explore the extent to which the average level of f_c changes with parameters, we show different heat maps in the square-lattice network and small-world network in Fig. 3.

It is easy to understand the heat map intuitively both from the horizontal and vertical axis, i.e., for each specified ρ_s , with the increase of ρ_r , f_c decreases, it is consistent with the previous analysis, and the same with results where ρ_r is fixed and ρ_s varies. Figs. 3(a), 3(b), and 3(c) reveal that the upper left area of the three heat maps is totally blue, which indicates that no cooperation is maintained under those conditions and colors change in the lower right area of the three heat maps. Furthermore, for $p = .4$, the phase transition becomes sharper in comparison with $p = .2$; namely, the cooperation frequency swiftly converges to 1 from 0 where there is no more an extended “stay” at a value between (0,1) with the slight fluctuation of the parameter pair (ρ_r, ρ_s) , and vice versa. For greater p , complex network systems undergo a sharper transition from pure cooperators ($f_c = 1$) to pure defectors ($f_c = 0$). And, we can observe the threshold of the emergence of cooperation according to the heat maps, i.e., the critical parameter for which the proportion of cooperators is greater than 0 (e.g., $(\rho_r, \rho_s) = (0, 0.25)$, $(0.15, 0.3)$ and $(0.2, 0.35)$ in Fig. 3(a)). Also, the threshold of the disappearance of defectors, i.e., the critical parameter for which the proportion of defectors equals 0 (e.g., $(\rho_r, \rho_s) = (0, 0.1)$, $(0.25, 0.15)$ and $(0.2, 0.2)$ in Fig. 3(d)). Comparing the heatmaps of $p = .4$ and $p = 1.0$, the red area expands towards the upper slightly, i.e., for p varying from 0.4 to 1.0, not much effect on f_c is observed in the figures. In Fig. 3(d), it indicates that for $p = .2$ in WS, cooperation can be maintained even under harsh conditions, i.e., ρ_r is larger than ρ_s , e.g., $(\rho_r, \rho_s) = (0.4, 0.2)$. For results in WS, we observe that the transition area, from pure defectors to pure cooperators, narrows as p increases, which is consistent with the results in SL. Furthermore, different from the results in SL, Figs. 3(d), 3(e), and 3(f) demonstrate that with the increase of p , the red area narrows, i.e., the conditions for pure cooperators become strict. The variance of p impacts the numbers of revengers and sufferers in the system, observed in Fig. 5, which is shown in subsection 3.5. *Evolution of numbers of revengers and sufferers over time.* It can result in the differences between the subplots under different p .

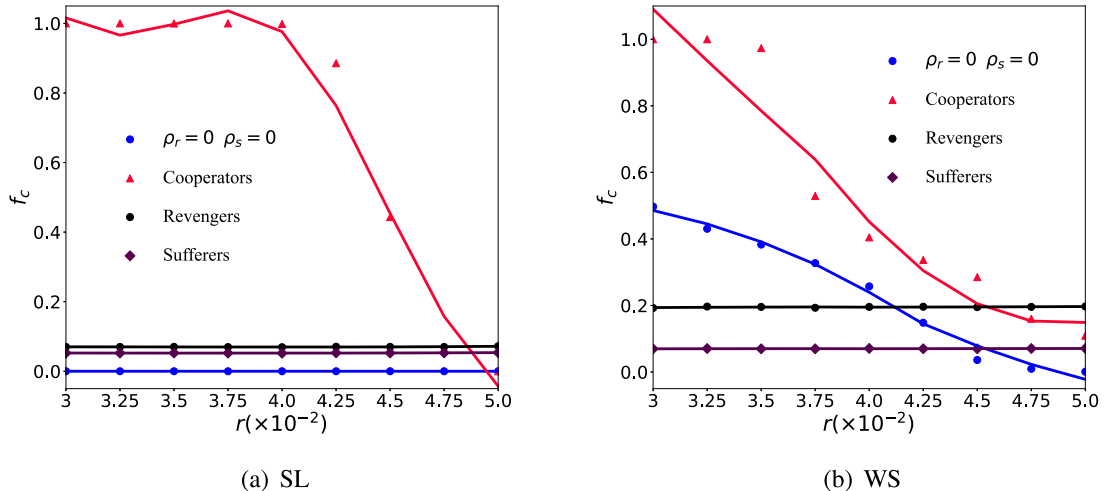


Fig. 4. Plots of frequency of different kinds of players against cost-to-benefit ratio. SL is generated by a square-lattice network with 40×40 nodes with periodical boundary conditions where each player has four neighbors. WS is generated by small-world networks where the reconnection probability is 0.3, the size of it is $N = 1600$, and $K = 10$. (ρ_r, ρ_s) is set as $(0, 0)$, $(0.2, 0.8)$ in each subplot. In Figs. 4(a) and 4(b), x-axis range varies from 0.03 to 0.05 and y-axis range is set as $[0, 1]$. In addition, p is set as 0.4 in two subplots. In two subplots, blue and red curves represent the ratio of cooperators under different parameters. We observe the cooperation frequency in each network until $t = 10^4$ to obtain the stable results of f_c .

3.4. Frequency of cooperation affected by cost-to-benefit ratio

We appoint $r = 0.02$ in the last part and the results signal that for relatively larger ρ_s and relatively smaller ρ_r , they remarkably boost the cooperation frequency in SL and WS. As we know, the parameter r in Eq.(1) reveals the strength of PDG, which directly influences the payoff of strategy pairs (C, D) and (D, C) , i.e., for greater r , the payoff of the unilateral cooperators becomes less, but that of the unilateral defectors becomes more. Therefore, we further probe whether the phenomenon maintains at the different values of r in this subsection. Significantly, the frequency of revengers and sufferers in Fig. 4 is referred to as the maximum frequency of revengers and sufferers. The percentages of cooperators and revengers are calculated by players adopting cooperation strategy and taking revenge behavior divided by the total number of players respectively since revenge and cooperative behavior are independent. Considering if f_c is maintained at a low or high level which leads to fewer shifts of strategies, it makes the steady results of the frequency of revengers (sufferers) after a long time evolution, like f_c , meaningless due to it often converges to 0.

As shown in Fig. 4, two subplots (a) and (b) exhibit a similar declining trend regarding f_c as the increase of r , namely, f_c decreases as r increases no matter in the square-lattice networks or the small-world networks. Moreover, with the benefit of the revenge mechanism, the cooperation frequency is remarkably enhanced in SL and WS, compared to the traditional mechanism under the same conditions, i.e., curves marked by red triangles are above curves marked by blue squares intuitively in the square-lattice network and small-world network, which proves the robustness of our mechanism. In Fig. 4(a), the red curve decreases sharply, i.e., f_c is sensitive to the minor variance of r . Though the maximal frequency of revengers and sufferers is maintained at a low level, around 7%, it remarkably boosts cooperation behaviors. In Fig. 4(b), except the drastic decrease of f_c when r varying from 3.5×10^{-2} to 3.75×10^{-2} , the variance of f_c is steady. Furthermore, the frequency of revengers and sufferers is around 20% and 7%, which indicates that one sufferer may be the target of multiple revengers, partly due to the critical parameter of WS $K = 10$. Moreover, in different r , the frequency of revengers and sufferers shows no difference, i.e., the maximum frequency in each independent simulation is close to a fixed value. Under the same conditions, we observe that the frequency of revengers almost equals the frequency of sufferers in SL, but in WS, the frequency of revengers is far greater than that of sufferers.

For the discrete data points, we apply the Savitzky-Golay filter to smooth the data (drawn by solid lines). Relevant methods are also taken in Fig. 6.

3.5. Evolution of numbers of revengers and sufferers over time

In the last subsection, we have given the different kinds of players in SL and WS against different r . To further explore and comprehend how revengers and sufferers impact f_c , we show the evolution of the numbers of revengers and sufferers in Fig. 5.

In Fig. 5(a), in the initial state, due to cooperators and defectors evenly distributed in the network, the number of revengers and sufferers is at a relatively high level. As time evolves, it shows a downward trend. For $p = .6$, revengers and sufferers disappear at round $t = 500$. In contrast, for $p = .3$, revengers and sufferers still exist in the system at a low proportion at $t = 2000$, due to the system not evolving into a pure state, where f_c converges to 0 or 1. In Fig. 5(b), different

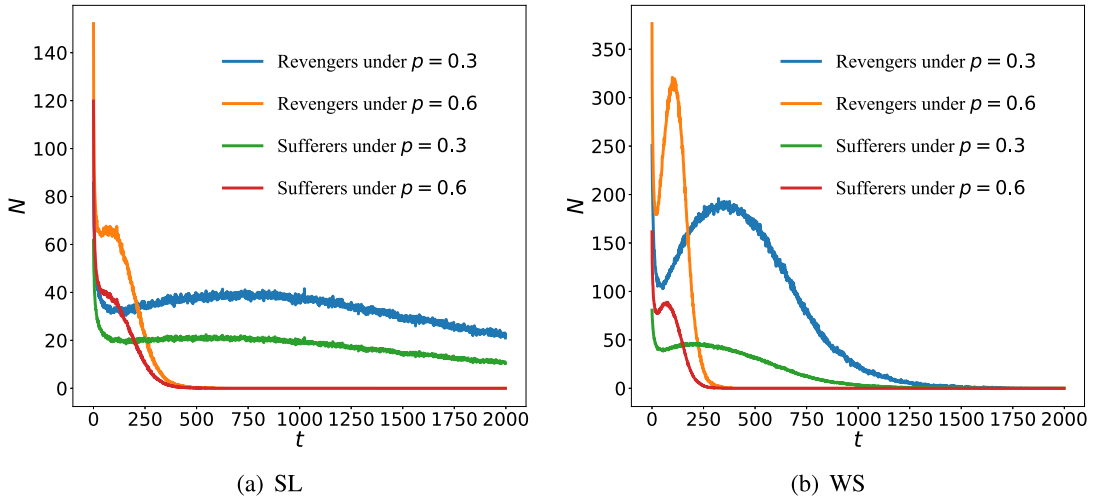


Fig. 5. Variance of numbers of revengers and sufferers against time. SL is a square-lattice network with $N = 40 \times 40$, and WS is formed by a small-world network with a reconnection probability of 0.3, the size of it is set as $N = 1600$ and $K = 10$. In Figs. 5(a) and 5(b), the parameter pairs (ρ_r, ρ_s) are set to $(0.2, 0.8)$. The range of each x-axis is set within the interval $[0, 2000]$, and y-axis of subplots (a) and (b) is set as $[0, 140]$ and $[0, 350]$ respectively. Additionally, the cost-to-benefit ratio r is set to 0.02 in the SL and WS. For comparison, we set $p = .3$ and $p = .6$ to observe relevant results.

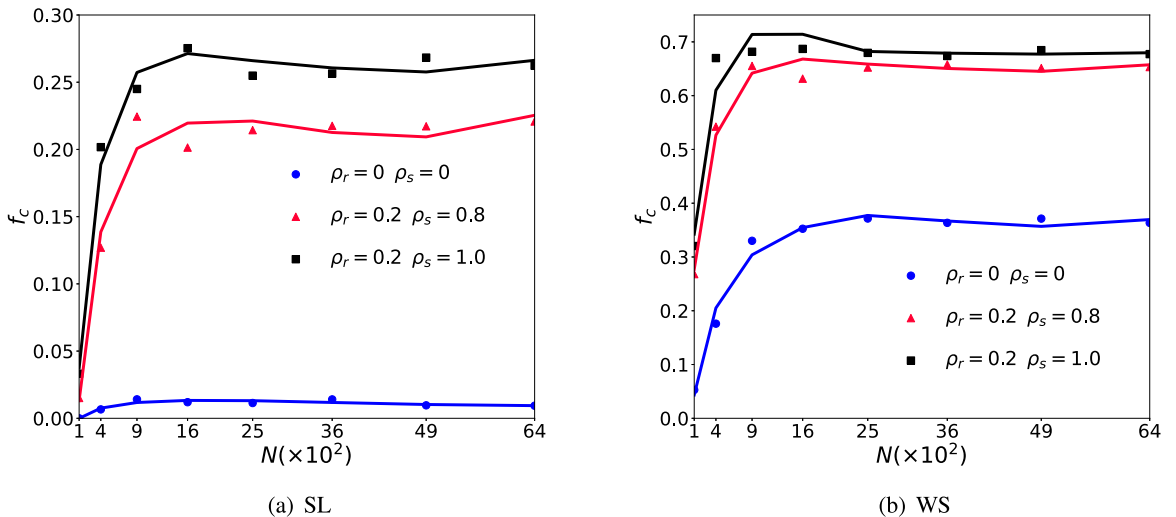


Fig. 6. Variance of frequency of cooperation against network size. The size of the network in Figs. 6(a) (SL) and 6(b) (WS), from left to right, is set as the square of 10 to 80, with step equals 10. The parameter pair (ρ_r, ρ_s) is set as $(0.2, 1.0)$ (black squares), $(0.2, 0.8)$ (red triangles) and $(0, 0)$ (blue circles). The y-axis is set as $[0, 0.3]$, and $[0, 0.7]$ respectively. In subplot (b), the parameter of WS is set as $K = 4$, and the reconnection probability is 0.3. Furthermore, we set $p = .1$ and $r = 0.02$ and 0.05 , respectively, for subplot (a) and subplot (b). We observe the cooperation frequency in each network until $t = 10^4$ to obtain the stable results of f_c .

from Fig. 5(a), for $p = .3$ and $p = .6$, there is a significant increase in the number of revengers and after reaching the highest point, it starts to decrease. Moreover, in Fig. 2, we have observed the phenomenon that after around $t = 100$, f_c stops its downward trend and turns up, which can be interpreted from the increase of revengers. We observe that for larger p , the existing time of revengers and sufferers is shorter in SL and WS. Moreover, we find that the maximum number of revengers and sufferers occurs in the initial phase, which indicates when the frequency of revengers and sufferers is greatest in the previous simulation.

3.6. Frequency of cooperation affected by network size

In the previous part, we all fix the network size as $N = 1600$; containing too fewer nodes may result in unreliability. Thus, to further verify the robustness of our model, the effect of network size on f_c is investigated under different (ρ_r, ρ_s) . We set the network size from 100 to 6400 for contrast in Fig. 6.

From Figs. 6(a) and 6(b), we observe that f_c increases with N for relatively small network size. Then, with the increase of N , f_c maintains at a steady frequency. In Fig. 6(a), for $N = 100$, defectors dominate the whole network in three different

parameter pairs; further, when $N = 400$, the red and black curves exhibit the striking upward trend, i.e., f_c is sensitive to the variance of relatively small N . For N larger than 900, f_c maintains around 0.2 and 0.25 respectively corresponding to (0.2,0.8), (0.2,1.0). Compared with the traditional mode, the red and blue curves achieve 20% to 25% improvement in f_c for N greater than 900. Similar phenomena are also observed in Fig. 6(b). The proposed model achieves around 30% improvement on f_c compared to the blue curve, and for $N \geq 400$ (black squares) and $N \geq 900$ (red triangles), f_c converges to 0.68 and 0.65 respectively corresponding to (0.2,0.8), (0.2,1.0).

4. Conclusion and discussion

In this study, we have studied the revenge-based mechanism in the prisoner's dilemma game with revengers and sufferers in SL and WS. Primarily, we suppose players whose current payoff is greater than 0 can execute revenge, and sufferers bear relevant losses in any case. Next, we give conditions for the execution of revenge and quantify the loss function to measure the strength of revenge, i.e., the second-order free riders are punished. Then, we utilize the Fermi strategy-updating rule, which provides a direct and easy-understanding way to measure the probability of updating strategies. In the simulation, the cost-to-benefit ratio r in the payoff matrix, the fraction of players p updating their strategies, the parameter pair (ρ_r, ρ_s) , are investigated to explore their effects on the cooperation frequency f_c to discover the potential factors which promote the emergence of cooperation. Notably, compared to the player without revenge, who is constrained in the traditional mechanism, facing the unilateral defection from its partner, the revenge mechanism rebalances the bilateral payoff. Therefore, the cooperation frequency is prompted by applying the revenge mechanism. Concretely, we can boost the cooperation frequency by changing the value of the parameter pair (ρ_r, ρ_s) within the appropriate intervals and the fraction ratio p . Results are comprehensible relating to the real world since with the benefit of revenge, which rebalances each player's payoff, i.e., the player who benefits from the variety of strategies shifting from mutual cooperation to unilateral defection is sanctioned, which effectively breaks the dilemma of cooperation and makes the emergence of cooperation possible. Furthermore, the effects of different cost-to-benefit ratios r on f_c in SL and WS have been studied, from which we get the conclusion that for different r on SL and WS, the cooperation frequency is facilitated, compared to the traditional mechanism. Subsequently, we explore the evolution of the numbers of revengers and sufferers over time, of which the results explain well the conclusions from the previous simulation. In the end, we examine the reliability on different network sizes and get the conclusion that for N larger than 900, the network size has almost no effect on the cooperation frequency, which illuminates the robustness of the proposed model.

In our work, the core of the revenge mechanism is the loss function, and we specify that the loss function has a linear relationship with the revenger's payoff in the current round, which is close to the real world and does not lose the generality, and we add the additional limit that whether it is greater than 0 determines the implementation of revenge. However, different forms of the loss function, such as the inverse proportional function, may trigger different results, and whether exist the general result will be the core of our research in the future. Furthermore, diverse strategy-updating rules, such as replicator dynamics, are also intriguing and mysterious, which may bring new discoveries. In the end, we expect our work can advance the interpretation of why cooperation behaviors exist widely in nature and human societies.

Data availability

Data will be made available on request.

Acknowledgments

This work was supported in part by the National Nature Science Foundation of China (NSFC) under Grant No. 62206230 and in part by the Humanities and Social Science Fund of Ministry of Education of the People's Republic of China under Grant No. 21YJCZH028.

References

- [1] C. Darwin, *On the Origin of Species*, Routledge, 2004.
- [2] K. Sigmund, *Games of Life: Explorations in Ecology, Evolution and Behavior*, Courier Dover Publications, 2017.
- [3] M. Archetti, K.J. Pienta, Cooperation among cancer cells: applying game theory to cancer, *Nat. Rev. Cancer* 19 (2) (2019) 110–117.
- [4] W.H. Press, F.J. Dyson, Iterated prisoner's dilemma contains strategies that dominate any evolutionary opponent, *Proc. Natl. Acad. Sci.* 109 (26) (2012) 10409–10413.
- [5] A. Rapoport, A.M. Chammah, *Prisoner's Dilemma: A Study in Conflict and Cooperation*, University of Michigan Press, 1965.
- [6] M. Doebeli, C. Hauert, Models of cooperation based on the prisoner's dilemma and the snowdrift game, *Ecol. Lett.* 8 (7) (2005) 748–766.
- [7] R. Kümmerli, C. Colliard, N. Fiechter, F. Russier, L. Keller, Human cooperation in social dilemmas: comparing the snowdrift game with the prisoner's dilemma, *Proc. R. Soc. B* 274 (1628) (2007) 2965–2970.
- [8] G. Szabó, C. Töke, Phase diagrams for the spatial public goods game with pool punishment, *Phys. Rev. E* 83 (3) (2001) 036101.
- [9] J. Quan, W. Yang, X. Li, J.-B. Yang, Social exclusion with dynamic cost on the evolution of cooperation in spatial public goods games, *Appl. Math. Comput.* 372 (2020) 124994.
- [10] G. Szabó, C. Töke, Evolutionary prisoner's dilemma game on a square lattice, *Phys. Rev. E* 58 (1) (1998) 69.
- [11] F. Shu, X. Liu, K. Fang, H. Chen, Memory-based snowdrift game on a square lattice, *Physica A* 496 (2018) 15–26.
- [12] A. Cassar, Coordination and cooperation in local, random and small world networks: experimental evidence, *Games Econ. Behav.* 58 (2) (2007) 209–230.

- [13] D.J. Watts, S.H. Strogatz, Collective dynamics of 'small-world' networks, *Nature* 393 (6684) (1998) 440–442.
- [14] F.C. Santos, J.M. Pacheco, Scale-free networks provide a unifying framework for the emergence of cooperation, *Phys. Rev. Lett.* 95 (9) (2005) 098104.
- [15] A.-L. Barabási, R. Albert, Emergence of scaling in random networks, *Science* 286 (5439) (1999) 509–512.
- [16] M. Feng, L.J. Deng, F. Chen, et al., The accumulative law and its probability model: an extension of the pareto distribution and the log-normal distribution, *Proc. R. Soc. A* 476 (2237) (2020) 20200019.
- [17] M. Feng, L. Deng, J. Kurths, Evolving networks based on birth and death process regarding the scale stationarity, *Chaos* 28 (8) (2018) 083118.
- [18] C.P. Roca, J.A. Cuesta, A. Sánchez, Effect of spatial structure on the evolution of cooperation, *Phys. Rev. E* 80 (4) (2009) 046106.
- [19] M.A. Nowak, Five rules for the evolution of cooperation, *Science* 314 (5805) (2006) 1560–1563.
- [20] J.L. Barker, J.L. Bronstein, M.L. Friesen, et al., Synthesizing perspectives on the evolution of cooperation within and between species, *Evolution* 71 (4) (2017) 814–825.
- [21] R.L. Trivers, The evolution of reciprocal altruism, *Q. Rev. Biol.* 46 (1) (1971) 35–57.
- [22] S. Righi, K. Takács, Social closure and the evolution of cooperation via indirect reciprocity, *Sci. Rep.* 8 (1) (2018) 1–9.
- [23] D.S. Wilson, A theory of group selection, *Proc. Natl. Acad. Sci.* 72 (1) (1975) 143–146.
- [24] X. Li, M. Jusup, Z. Wang, H. Li, L. Shi, Punishment diminishes the benefits of network reciprocity in social dilemma experiments, *Proc. Natl. Acad. Sci.* 115 (1) (2018) 30–35.
- [25] Z. Wang, A. Szolnoki, M. Perc, Interdependent network reciprocity in evolutionary games, *Sci. Rep.* 3 (1) (2013) 1183.
- [26] H. Ohtsuki, C. Hauert, E. Lieberman, M.A. Nowak, A simple rule for the evolution of cooperation on graphs and social networks, *Nature* 441 (7092) (2006) 502–505.
- [27] M. Fu, W. Guo, L. Cheng, S. Huang, History loyalty-based reward promotes cooperation in the spatial public goods game, *Physica A* 525 (2019) 1323–1329.
- [28] P. Zhu, X. Wang, D. Jia, Y. Guo, S. Li, C. Chu, Investigating the co-evolution of node reputation and edge-strategy in prisoner's dilemma game, *Appl. Math. Comput.* 386 (2020) 125474.
- [29] B. Pi, Y. Li, M. Feng, An evolutionary game with conformists and profiteers regarding the memory mechanism, *Physica A* 597 (2022) 127297.
- [30] B. Pi, Z. Zeng, M. Feng, J. Kurths, Evolutionary multigame with conformists and profiteers based on dynamic complex networks, *Chaos: Interdiscip. J. Nonlinear Sci.* 32 (2) (2022) 023117.
- [31] Z. Zeng, Y. Li, M. Feng, The spatial inheritance enhances cooperation in weak prisoner's dilemmas with agents' exponential lifespan, *Physica A* 593 (2022) 126968.
- [32] J. Quan, X. Li, X. Wang, The evolution of cooperation in spatial public goods game with conditional peer exclusion, *Chaos: Interdiscip. J. Nonlinear Sci.* 29 (10) (2019) 103137.
- [33] Z.-H. Deng, Z.-R. Wang, H.-B. Wang, L. Xu, The evolution of cooperation in multi-games with popularity-driven fitness calculation, *Chaos, Solitons Fractals* 151 (2021) 111298.
- [34] A. Li, L. Zhou, Q. Su, S.P. Cornelius, Y.Y. Liu, L. Wang, S.A. Levin, Evolution of cooperation on temporal networks, *Nat. Commun.* 11 (1) (2020) 1–9.
- [35] U. Alvarez-Rodriguez, F. Battiston, G.F. de Arruda, Y. Moreno, M. Perc, V. Latora, Evolutionary dynamics of higher-order interactions in social networks, *Nat. Hum. Behav.* 5 (5) (2021) 586–595.
- [36] Q. Li, G. Zhao, M. Feng, Prisoner'S dilemma game with cooperation-defection dominance strategies on correlational multilayer networks, *Entropy* 24 (6) (2022) 822.
- [37] H.-X. Yang, X. Chen, Promoting cooperation by punishing minority, *Appl. Math. Comput.* 316 (2018) 460–466.
- [38] X. Chen, A. Szolnoki, M. Perc, Competition and cooperation among different punishing strategies in the spatial public goods game, *Phys. Rev. E* 92 (1) (2015) 012819.
- [39] Q. Song, Z. Cao, R. Tao, W. Jiang, C. Liu, J. Liu, Conditional neutral punishment promotes cooperation in the spatial prisoner's dilemma game, *Appl. Math. Comput.* 368 (2020) 124798.
- [40] J.-F. Wang, J.-L. Guo, A synergy of punishment and extortion in cooperation dilemmas driven by the leader, *Chaos, Solitons Fractals* 119 (2019) 263–268.
- [41] B. Rockenbach, M. Milinski, The efficient interaction of indirect reciprocity and costly punishment, *Nature* 444 (7120) (2006) 718–723.
- [42] D. Helbing, A. Szolnoki, M. Perc, G. Szabó, Punish, but not too hard: how costly punishment spreads in the spatial public goods game, *N. J. Phys.* 12 (8) (2010) 083005.
- [43] A. Dreber, D.G. Rand, D. Fudenberg, M.A. Nowak, Winners don't punish, *Nature* 452 (7185) (2008) 348–351.
- [44] J. Wang, W. Chen, F. Yu, J. He, W. Xu, Wealth-based rule favors cooperation in costly public goods games when individual selection is inevitable, *Appl. Math. Comput.* 414 (2022) 126668.
- [45] L. Mieth, A. Buchner, R. Bell, Moral labels increase cooperation and costly punishment in a prisoner's dilemma game with punishment option, *Sci. Rep.* 11 (1) (2021) 1–13.
- [46] J. Elster, Norms of revenge, *Ethics* 100 (4) (1990) 862–885.
- [47] R. Axelrod, W. Hamilton, The evolution of cooperation, *Science* 211 (4489) (1981) 1390–1396.
- [48] M.A. Nowak, K. Sigmund, Tit for tat in heterogeneous populations, *Nature* 355 (6357) (1992) 250–253.